Physica B ■ (■■■■) ■■■–■■■

Contents lists available at ScienceDirect

Physica B

journal homepage: www.elsevier.com/locate/physb

Magnetoimpedance studies on as-quenched $Fe_{66-x}Co_xNi_7Si_7B_{20}$ (x=0, 33 and 66) ribbons

Ganesh Kotagiri, G. Markandeyulu [1]

Advanced Magnetic Materials Laboratory, Department of Physics, Indian Institute of Technology Madras, Chennai 600036, India

ARTICLE INFO

Keywords:
Magnetoimpedance
METGLAS
Amorphous magnetic materials
Magnetic anisotropy

ABSTRACT

Magnetoimpedance (MI) has been investigated in the as quenched $Fe_{66-x}Co_xNi_7Si_7B_{20}$ (x=0, 33 and 66) ribbons. In plane anisotropy was present in as-quenched x=0, 33 and 66 ribbons. The largest MI values for x=0, 33 and 66 ribbons are 25% (at 7 MHz), 26% (at 8 MHz) and 45% (at 8 MHz) respectively. Largest MI values increased with increasing Co due to reduced magnetic anisotropy. Maximum MI values reduced at higher frequencies due to increased anisotropy fields.

1. Introduction

Amorphous materials are suitable candidates for magnetic field sensor applications [1,2]. METGLAS is attracting researchers for several years due to its high mechanical strength and soft magnetic properties [3,4]. Magnetoimpedance (MI) is the change in impedance of a soft ferromagnetic material when it is subjected to static magnetic field, through changes in transverse permeability μ_T (related with skin effect [5]) and is defined as $(\Delta Z/Z)\% = Z(H) - Z(H_{max})/Z(H_{max}) \times 100$, where $Z(H)$ is the impedance at a field H and $Z(H_{max})$ is the impedance at a maximum field in the measurement. METGLAS has been reported as one of the preferred candidates for biosensors due to its higher sensitivity [6]. In our laboratory, MI studies on METGALS based ribbons, $Co_{68}Fe_5Si_{12}B_{15}$ and $Co_{68}Fe_5Nb_{12}B_{15}$, have been reported [4,7]. The negative magnetostriction resulting in the formation of transverse (to the length of ribbon) magnetic domains in these ribbons aids enhancement of MI [8]. At low frequencies, transverse magnetization changes through domain wall motion and rotation of the moment takes place after the applied static field (H_{ext}) is larger than the anisotropy field (H_k) [9]. At higher frequencies, skin effect is significant and the domain wall-motion gets damped due to eddy currents whence moment rotation contributes to the magnetization process [9] and MI reduces due to large skin effect due to reduction in μ_T [10,11]. In order to investigate MI in a relatively magnetically soft ribbon, in the present studies, $Fe_{66-x}Co_xNi_7Si_7B_{20}$ (x=0, 33 and 66) were considered. Ni and Si were substituted for a part of Fe to reduce magnetostriction and enhance magnetic softness [8,12–15] with a view to improve the sensitivity and subsequently Co was replaced with Fe to obtain very large and sensitive MI [9]. In this paper, the structural and magnetization along with MI studies on the above mentioned ribbons are presented.

2. Experimental details

$Fe_{66-x}Co_xNi_7Si_7B_{20}$ (x=0, 33 and 66) alloys were prepared by arc melting with elements of purity, Fe – 99.97%, Co – 99.999%, Ni – 99.97%, Si – 99.995% and B – 99.5%, all procured from Alfa Aesar, in argon atmosphere. Ribbons were prepared by a single Cu-roller melt spinning technique in argon atmosphere. Cu disk of diameter 18 cm rotating at a speed of 2800 rpm was employed. All three ribbons were about 1–2 m long (the length is referred to as the axis of the ribbon, subsequently), 0.9 mm wide and 30 μm thick. The as-quenched ribbons were found to be amorphous through powder XRD studies carried out, employing a Philips PANalytical X'pert PRO X-ray diffractometer with an X'celerator detector and employing Cu Kα radiation. DSC (NETZSCH, DSC 204 F1 phoenix) studies with a heating rate of 10 °C/min were carried out to determine crystallization temperatures. Impedance measurements were carried out using a HP-4192A impedance analyzer with an alternating current of 10 mA and in the frequency range 1–13 MHz, on 5 cm long ribbons. The external static magnetic field up to ± 100 Oe was applied employing Helmholtz coils. The probe (alternating current) current and applied static fields were along the axis of the ribbon. Surface morphology studies were carried out by HRSEM (HITACHI, MODEL S-4800). Selected area electron diffraction (SAED) studies were carried out using a Philips CM12 TEM with an accelerating voltage of 120 kV on an ion-beam milled (x=66) ribbon. Magnetization measurements were carried out on square shaped ribbons using a VSM (MicroSense, Model EZ-9),

E-mail address: mark@physics.iitm.ac.in (G. Markandeyulu).
[1] Fax: +914422570509/22574852.

http://dx.doi.org/10.1016/j.physb.2014.03.049
0921-4526/© 2014 Published by Elsevier B.V.

both in the longitudinal and transverse directions to the axis of the ribbon.

3. Results and discussion

The bulk amorphous nature of the as-quenched ribbons was examined by XRD in the powder mode (Fig. 1(a)). The results of the DSC (thermal analysis) studies are shown in Fig.1(b). The crystallization temperatures of $x=0$, 33 and 66 amorphous ribbons are seen to be 542, 565 and 550 °C respectively. Fig. 2 shows the microstructures (HRSEM micrographs) of the as-quenched ribbons where amorphous nature of $x=0$ and 33 ribbons is seen. Square shaped grains of sizes in the range 100–500 nm are seen in amorphous matrix in the case of $x=66$ ribbons. Grazing incident XRD (GIXRD) (angle of incidence of the X-ray beam was in the range 1–5°) taken to observe the surface grain structure of this ribbon did not reveal any crystallinity of these grains (as shown in Fig. 3). To identify the abnormal structure of these grains which were embedded in the amorphous matrix in $x=66$ ribbon, SAED studies on these areas were carried out and the micrograph is shown in Fig. 4(a) (shows the corresponding diffraction pattern of $x=66$ bright field image). Fig. 4(b) shows the reflection from the diffraction pattern and from the figure it is clear that the grains which were embedded in amorphous matrix of $x=66$ ribbon might be HCP crystal structure with zone axis of $[01\bar{1}1]$.

Fig. 5 shows *M–H* curves in longitudinal and transverse directions to the ribbon axis. It is clear that the saturation magnetization decreased with increasing Co as per the behavior in Fe–Co alloys. In addition, magnetic anisotropy is observed in the plane of the ribbons (the field required to saturate the moments is different in longitudinal and transverse directions). The transverse direction is seen to be the hard direction in all ribbons. The anisotropy is seen to be smaller for Co containing ribbons than for $x=0$ (Fe-based) ribbon. However, no systematic variation in anisotropy is observed.

Fig. 6 shows the MI profile at frequencies at which MI is the largest for three ribbons. The largest MI values for $x=0$, 33 and 66 ribbons are 25% (at 7 MHz), 26% (at 8 MHz) and 45% (at 8 MHz) respectively. The increase in MI with increasing Co is attributed to decreasing anisotropy. The maximum MI value in $x=66$ ribbon is seen to be significantly large compared to those reported for $Co_{68}Fe_5Si_{12}B_{15}$ and $Co_{68}Fe_5Nb_{12}B_{15}$ amorphous ribbons [4,7]. Inclusion of Ni in the alloy seems to have reduced the anisotropy and hence, increase in the MI. A very clear double peak behavior is observed in the $x=66$ ribbon indicating the presence of a transverse domain structure [10]. A careful observation of the SEM image of the $x=66$ ribbon shows that the square shaped grains gather themselves in such a way that they can together be treated as a pseudo-transverse domain pattern. As both probe current and applied static field are perpendicular to the transverse domain pattern at $H_{ext}=H_k$ (anisotropy field) μ_T is significantly large which causes a large change in the impedance [9]. The MI curves, expanded in the field range −12 Oe to 12 Oe, are shown in Fig. 7. Double peak behavior is observed in all the ribbons, though not much pronounced in some. Anisotropy fields (H_k) are seen to increase with increasing driving frequency for all the three ribbons. Due to larger H_k, μ_T decreases causing MI to decrease at higher frequencies [10,11]. The largest *MI* value is seen to increase with increasing driving frequency and reach a maximum and then decreases subsequently at higher frequencies (Fig. 8). This is due to

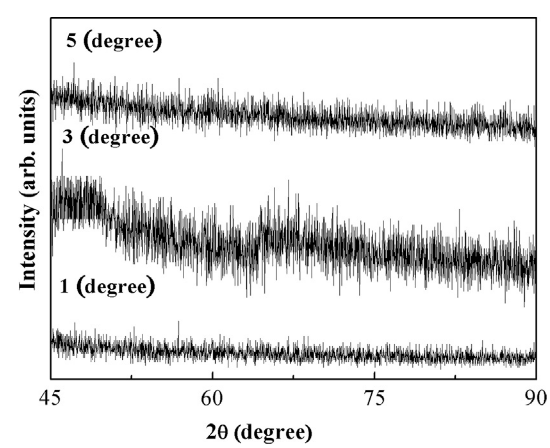

Fig. 3. GIXRD patterns of as-quenched $x=66$ ribbon.

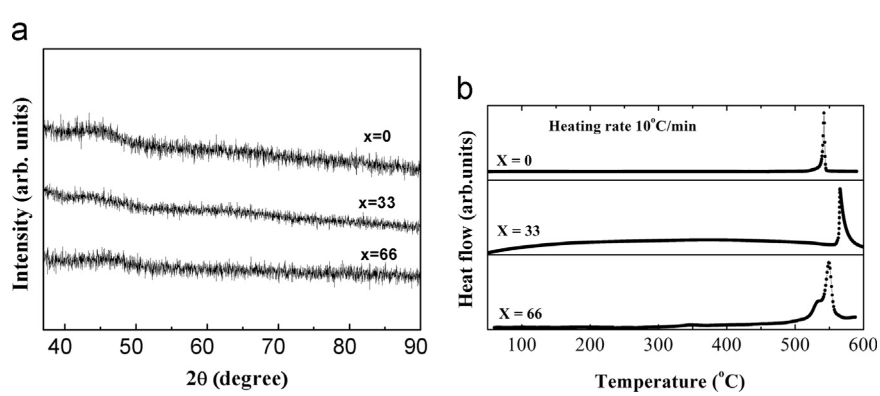

Fig. 1. XRD patterns (a) and DSC of as-quenched $x=0$, 33 and 66 ribbons (b).

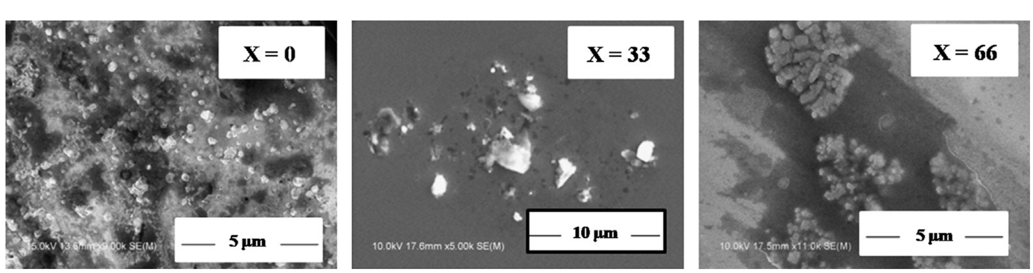

Fig. 2. HRSEM micrographs of as-quenched $x=0$, 33 and 66 ribbons.

Please cite this article as: G. Kotagiri, G. Markandeyulu, Physica B (2014), http://dx.doi.org/10.1016/j.physb.2014.03.049